Enhanced Computer Modeling of Cardiac Action Potential Dynamics using Experimental Data-Based Feedback

Laura M Muñoz[1], Niels F Otani[1]

[1]Department of Biomedical Sciences, Cornell University, Ithaca, USA

Abstract

Mathematical models of cardiac action potential (AP) dynamics are useful for studying the formation of dynamically significant patterns such as alternans and conduction block. A closed-loop observer is an augmented version of a mathematical model, in which experimental data are supplied to the model through feedback. In this study, tools for observer analysis were applied to a two-variable Karma model of AP dynamics. For a single-cell system, it was confirmed that membrane potential data could be used to reconstruct the system state, and that Luenberger feedback could stabilize the observer. Next an observer with a 1D geometry was tested with microelectrode membrane-potential data from a 2.1cm in vitro canine Purkinje fiber. It was shown that the observer produced more accurate AP duration (APD) estimates than the model by itself. These reconstructed quantities could be used to provide enhanced information to anti-tachyarrhythmic stimulus protocols that depend on real-time measurements.

1. Introduction

Research into the mechanisms underlying lethal cardiac arrhythmias has been facilitated by a variety of experimental measurement techniques, including electrode recordings, optical mapping, and patch clamping. Typically, experimentalists encounter limits in the number of quantities and measurement sites that they can monitor during an *in vitro* or *in vivo* experiment. A complementary approach is to perform computer simulation studies on relevant mathematical models, such as ion-channel models. These models allow researchers to examine the interplay between variables and the formation of arrhythmias more thoroughly than is possible in a laboratory setting. One way to combine data collection and mathematical modeling is to build a closed-loop observer, a type of data-driven mathematical model that has been used frequently in engineering studies but has been applied less often to models of AP dynamics [1, 2]. A possible benefit of an observer is that it could serve as a set of "virtual sensors" that generates estimates of membrane potentials away from sensing electrodes or allows ionic fluxes to be reconstructed from membrane-potential data. Another important application is using an observer to improve the performance of a real-time feedback algorithm that computes timings of anti-tachyarrhythmic stimuli based on recent measurements of cardiac activity.

In the present study, an observer was designed by augmenting the two-variable Karma model [3, 4] with Luenberger-type feedback. Observability Grammians were computed for a single-cell Karma model to determine whether the membrane potential variable or the refractory variable is the better choice for reconstructing the initial state of the model. Next, a restricted search of stabilizing observer gain values was used to determine gains that were optimal in the sense of minimizing the 2-norm of the closed-loop eigenvalues of the single-cell model. These results were extended to a more practical case, wherein a 106-cell observer was applied to membrane-potential data from microelectrodes embedded in a 2.1cm *in vitro* canine Purkinje fiber.

2. Methods

The two-variable Karma model [3,4] was chosen, due to its simplicity, as the basis for the observer. The equations were

$$V_t = \gamma V_{xx} + \frac{1}{\tau_V} f(V,n) - c\, i, \quad n_t = \frac{1}{\tau_n} g(V,n), \quad (1)$$

where $V(x,t)$ is the membrane potential (in mV) at location x at time t, $n(x,t)$ is the refractory variable (dimensionless), and $i(x,t)$ is the stimulus current (in μA cm^{-2}). f and g are defined as

$$f(V,n) = -V - V_b + (\nu - n^M)\left(\sum\nolimits_{j=0}^{3} c_j V^j\right),$$

$$g(V,n) = \frac{1}{b}\theta(V - V_n) - n,$$

where $\theta(\cdot)$ is the Heaviside function. No-flux boundary conditions, $V_x(0,t) = V_x(L,t) = 0$, were assumed. Initial parameter values were chosen similarly to those from

a previous study [5], but were adjusted to give a better match to measured conduction velocities, resulting in: $\gamma = 0.005\text{cm}^2\ \text{ms}^{-1}$, $\tau_V = 0.7$ms, $c = 1\text{cm}^2\ \mu\text{F}^{-1}$, $\tau_n = 170$ms, $V_b = 90$mV, $\nu = 4$, $M = 10$, $b = 0.7059$, $V_n = -65$mV, $c_0 = 107.8831$mV, $c_1 = -0.1319$, $c_2 = -0.0465\text{mV}^{-1}$, and $c_3 = -3.52 \times 10^{-4}\ \text{mV}^{-2}$. Eliminating the dependence on x produced a single-cell version of the equations.

Eq. (1) was discretized with a forward-Euler scheme, using $F_{xx}(x,\cdot) \approx (F(x+\Delta x,\cdot) - 2F(x,\cdot) + F(x-\Delta x,\cdot))/(\Delta x)^2$. Default step sizes were $\Delta t = 0.008$ms and $\Delta x = 0.02$cm. Cells and fibers simulated in Matlab with the Karma model were paced by applying a periodic train of rectangular pulses to cell 1 with a stimulus value of $-1120\ \mu\text{A cm}^{-2}$, and a stimulus duration of 1ms.

For an N-cell fiber, the state vector is

$$z(k) = [V_1(k)\ \ldots\ V_N(k)\ n_1(k)\ \ldots\ n_N(k)]^T,$$

with discrete time index $k \in \{0,1,2,\ldots\}$. Suppose that $z_o(k)$ is a known solution to the discretized Eq. (1) for a reference input $i_o(k)$, z^{act} is a vector of real-world counterparts to the model-based elements of z, and that $\tilde{z} = z_o - z$, with $\tilde{z}^{\text{act}} = z_o - z^{\text{act}}$. It was assumed that the vector of measured variables available for the observer design could be written as $y^{\text{act}} = Cz^{\text{act}}$, where $C \in \mathbb{R}^{N_o \times 2N}$ and $N_o \in \{1,2,\ldots,2N\}$. The observer error was defined as $e = \tilde{z}^{\text{act}} - \tilde{z}$, and the observer feedback gain was chosen as a matrix $L \in \mathbb{R}^{2N \times N_o}$. The Karma model was converted to a closed-loop observer by adding the Luenberger-type feedback term $\Delta t LCe(k)$ to the discretized version of Eq. (1).

For the idealized case where the measured and modeled stimulus currents are identical and $z^{\text{act}}(k)$ satisfies the Karma model equations, the observer error dynamics linearized about z_o have the form $e(k+1) = (A(k) - LC)e(k)$, where $A(k)$ is the time-varying Jacobian for the open-loop system. The system integrated over one basic cycle length (BCL) is $e_{j+1} = \left(\prod_{k=k_j}^{k_j-1+BCL/\Delta t}(A(k) - LC)\right) e_j = A_{\text{int}} e_j$. Here, k_j is the time index at the start of the j^{th} BCL.

For the single-cell model, observability Grammians were computed to determine which of the variables, V or n, is a better choice for reconstructing the state from an available measurement. The standard observability Grammian definition for linear-time-varying systems was applied to a non-dimensionalized version of $A(k)$ derived previously [6], assuming $L = 0$. Two cases were considered: in the first, only measurements of the membrane potential were used (i.e., $C = [1\ \ 0]$), and in the second, only measurements of the refractory variable were used ($C = [0\ \ 1]$).

Keeping the eigenvalues of $A(k) - LC$ inside the unit circle is not a sufficient condition for system stability. Hence, to quantify the effect of different feedback configurations for $L \neq 0$, a methodology was established for computing the eigenvalues $\lambda_1, \ldots, \lambda_{2N}$ of A_{int}, which is time-invariant when evaluated on a periodic z_o trajectory. First, a fixed point of the time-integrated Karma model was estimated using a Newton-Krylov solver [7]. A_{int} was computed using a finite-difference approach [7] modified to apply perturbations scaled relative to the magnitude of each state-vector element. A central-difference method was then applied to reduce the impact of errors in the fixed-point estimate on the Jacobian [8]. Eigenvalues were determined with the `eig` function in Matlab.

To test the applicability of the observer concept, data were obtained from a December 17, 2002 *in vitro* experiment on a 2.1cm beagle Purkinje fiber. The fiber was paced periodically from one end with a biphasic electrode, and membrane potential recordings were made with six microelectrodes spaced approximately evenly along the fiber, with a 0.001s sampling interval. Raw data were processed by subtracting out the vertical offsets of each of the six signals, and converting to voltage units by assuming a resting potential of -90mV and a base-to-peak amplitude of 125mV. The data were zero-order-hold interpolated when used in computer simulations.

This experimental setup was mimicked through simulations of the Karma model with a 106-cell fiber, with initial condition $V = -85$mV and $n = 0$ for all cells. The microelectrodes were assumed to be located at cells 16, 31, 46, 61, 76, and 91 ($x = 0.32$, 0.62, 0.92, 1.22, 1.52, and 1.82cm). Tests were conducted to determine whether membrane-potential measurements could be approximated using feedback from only some of the sensor signals. To quantify the performance of the observer, an APD error measure was calculated as $APDE = \frac{1}{3}\sum_{m\in\{31,61,91\}} \frac{1}{J}\sum_{j=1}^{J} |APD^{\text{act}}_{m,j} - APD_{m,j}|$, where m is the cell index, j is the AP index, J is number of APs in the range of 3000 to 4100ms, and the quantities inside the absolute value are the measured and observer-derived APDs, respectively. APDs were judged by the crossings of the rising and falling edges with the line $V = -78$mV, which was chosen to approximate APD_{90} for this data set.

3. Results

$A(k)$ was first evaluated on a trajectory produced by simulating the single-cell (open-loop) model with a BCL of 230ms. Fig. 1 shows that the resulting minimum singular values of the observability Grammian are greater for the case of measuring V than for measuring n. This comparison holds for both shorter (Fig. 1(a)) and longer (Fig. 1(b)) Grammian time ranges.

In Fig. 2(a), it can be seen that for a search of L_{11} in the range of -1.7 to 0, increasing by increments of 0.1, with $L_{21} = 0$, a minimum in the two-norm of the eigenvalue

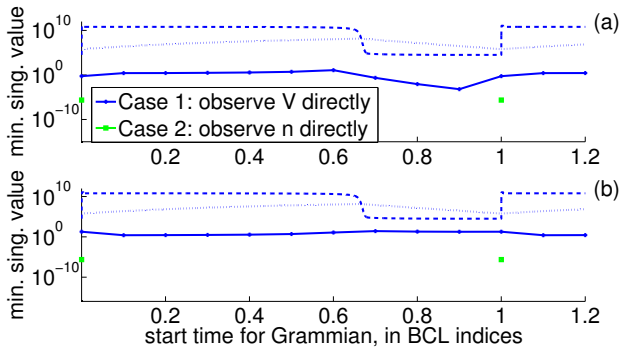

Figure 1. Minimum singular values of observability Grammians for the single-cell model, with a Grammian time window of: (a) 1/10 BCL (23ms) (b) one BCL (230ms). Crosses indicate an output vector of $C = [1 \quad 0]$ and squares indicate $C = [0 \quad 1]$. There are only two squares per subplot, since for $C = [0 \quad 1]$ the majority of the minimum singular values are very close or equal to zero. Scaled versions of the corresponding V (dashed) and n (dotted) trajectories are shown for reference.

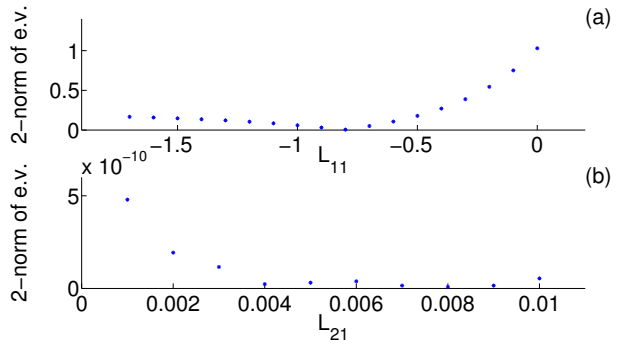

Figure 2. Two-norms of eigenvalue vectors (e.v.), showing the impact of different valuations of the gain vector $L = [L_{11} \; L_{21}]^T$ on a single-cell model with a BCL of 230ms: (a) norms for selected values of L_{11}, with $L_{21} = 0$, (b) norms for selected values of L_{21}, with $L_{11} = 0$.

vector $[\lambda_1 \; \lambda_2]^T$ was attained for $L_{11} = -0.8$. Setting the other gain element to zero and testing L_{21} from 0.001 to 0.01, increasing by increments of 0.001, revealed two local minima in the eigenvalue norm, with the smallest norm achieved at $L_{21} = 0.008$, as shown in Fig. 2(b). Values in the range $L_{11} > 0$ or $L_{21} < 0$ sometimes produced convergent fixed-point estimates, but did not stabilize the observer about a 1:1 trajectory of the Karma model. Increasing L_{21} through 0, 0.0002, 0.0004 for $L_{11} = -0.8$ caused the two-norm to decrease from 0.0055 to 1.4456×10^{-5}.

For the 106-cell fiber, tested configurations included gains of the form $L_{m,m} = \xi_1$, with all other entries zero (signifying V_m-to-V_m feedback), and $L_{N+m,m} = \xi_2$, all other entries zero (V_m-to-n_m feedback), with $m \in \{16, 46, 76\}$. The values of the constants $\xi_{1,2}$ were adjusted by trial and error. Feeding back n was not tested, since n is not measurable. Figs. 3(a) and (b) show that the feedback signal was on the order of the pacing pulse, and eventually settled into a nearly periodic pattern. Comparing Figs. 3(c),(e) to (d),(f), it can be seen that the closed-loop case provided more accurate estimates of membrane potentials than the model by itself. The closed-loop observer also reduced APDE from 69.5ms to 12.9ms. However, it greatly overestimated the plateau potential, which could most likely be improved through better calibration of the model. Setting $\xi_1 = 0$, results of V_m-to-n_m feedback were inferior to those of Fig. 3 for $\xi_2 = 0.0005$, while values $\xi_2 \geq 0.0008$ appeared to destabilize the observer.

4. Discussion and conclusions

The observability results demonstrate that, for the single-cell Karma model, it is more useful to measure V than n in order to reconstruct the state of the system. This is fortunate, considering that membrane-potential measurements are generally the only type that can be easily obtained from real tissue, whereas n is not a practically measurable quantity. The single-cell results in Fig. 2 showed that V-based observer feedback applied to either the V- or n-dynamics could at least stabilize the system about a 1:1 trajectory. This gave confidence that the observer could be used to track real membrane-potential measurements.

The fiber results in Fig. 3 established that Luenberger observer feedback can be used to force the Karma model to follow a trajectory, namely a selected set of microelectrode action-potential measurements, that is not native to the model. Due to the absence of V_m-to-n_m feedback, the scheme is similar to that of Rappel, *et al.* [5], where V from the previous period has been replaced in the present study by the measured membrane potential. Here, feedback was applied for a different purpose, to reconstruct data rather than to eliminate alternans [5].

One distinction from other works involving Luenberger observers for APD or AP models [1, 2] is that here, the observer was applied to real data. Another difference is that previous studies [1,2] used linear-time-invariant (LTI) methods (e.g., pole placement) that generated one observer feedback pulse per BCL. This study takes advantage of the fact that, unlike a feedback-controlled stimulator that must interact with real tissue, an observer has fewer restrictions on how and when feedback signals are applied. A disadvantage is that the design problem of choosing L to affect the eigenvalues of A_{int} is generally more challenging than the typical LTI case.

This study was intended as a starting point for further investigations into observer design. The design and analysis tools could be extended to the multicellular case to obtain

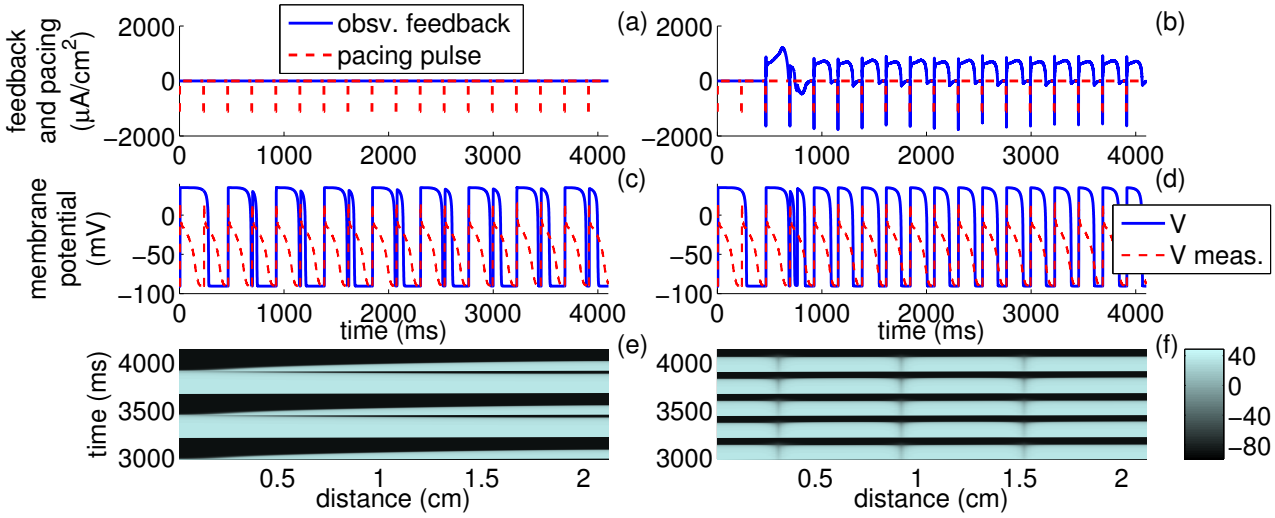

Figure 3. Comparison of open-loop model ((a),(c),(e)) and closed-loop observer ((b),(d),(f)) with $\xi_1 = -25$, $\xi_2 = 0$, and BCL = 230ms. In the closed-loop case, V_m-to-V_m feedback (initiated at 450ms) was applied at 3 of 6 measurement locations, at cells 16, 46, and 76 ($x = 0.32$, 0.92, and 1.52cm). (a),(b): observer feedback signal vs. time at cell 46, along with pacing pulse applied to cell 1 of the simulated system. (c),(d): simulated and measured membrane potentials vs. time at cell 61 ($x = 1.22$cm), which was a non-feedback location. (e),(f): simulated membrane potentials vs. time and distance along the fiber. In (b) and (d), the remaining feedback or AP time-series curves were similar but were omitted for brevity.

insights into best sensor placement. If the observability results in Fig. 1 turn out to hold for ion-channel models, then measurements of V can be used to reconstruct ionic flows through the cell membrane. To be practically useful, observers must be designed to work with more complicated measured AP patterns, such as alternans.

Overall, the results show that a closed-loop observer is a viable approach for estimating variables (in this case V and n) at locations away from the measurement electrodes. Beyond data reconstruction, the observer could be used to enhance the performance of an alternans-suppressing feedback controller by providing estimates of unmeasurable variables. The observer also provides a complementary method to model-parameter estimation, since accurate calibration of parameters cannot generally address all discrepancies between modeled and measured behavior.

Acknowledgements

The authors would like to thank Professor Robert Gilmour, Jr. and Mark Riccio for providing the Purkinje-fiber data used in this study. The project described was supported by Award Number R01HL089271 from the National Heart, Lung, And Blood Institute. The content is solely the responsibility of the authors and does not necessarily represent the official views of the National Heart, Lung, And Blood Institute or the National Institutes of Health.

References

[1] Dubljevic S. Optimal boundary control of cardiac alternans. Int J Robust Nonlinear Control 2009;19:135–150.

[2] Garzón A, Grigoriev RO, Fenton FH. Controllability of cardiac alternans in Purkinje fibers. To be submitted to Phys Rev Lett.

[3] Karma A. Spiral breakup in model equations of action potential propagation in cardiac tissue. Phys Rev Lett 1993; 71(7):1103–1106.

[4] Karma A. Electrical alternans and spiral wave breakup in cardiac tissue. Chaos 1994;4(3):461–472.

[5] Rappel WJ, Fenton FH, Karma A. Spatiotemporal control of wave instabilities in cardiac tissue. Phys Rev Lett July 1999; 83(2):456–459.

[6] Muñoz LM, Stockton JF, Otani NF. Applications of control theory to the dynamics and propagation of cardiac action potentials. Ann Biomed Eng 2010;38(9):2865–2876.

[7] Kelley CT. Solving Nonlinear Equations with Newton's Method. Number 1 in Fundamentals of Algorithms. Philadelphia: SIAM, 2003.

[8] Li M, Otani NF. Ion channel basis for alternans and memory in cardiac myocytes. Ann Biomed Eng 2003;31:1213–1230.

Address for correspondence:

Laura Muñoz
Box 17 Veterinary Research Tower
Cornell University
Ithaca, NY 14853
LM288@cornell.edu